British Journal of Pharmacology (2008) 155, 641–654

0007–1188/08 $32.00
www.brjpharmacol.org

RESEARCH PAPER

Benzylidene derivatives of andrographolide inhibit growth of breast and colon cancer cells *in vitro* by inducing G_1 arrest and apoptosis

SR Jada[1,6], C Matthews[2], MS Saad[3], AS Hamzah[4], NH Lajis[5], MFG Stevens[2] and J Stanslas[1,5]

[1]*Department of Biomedical Sciences, Faculty of Medicine and Health Sciences, Universiti Putra Malaysia, Serdang, Selangor, Malaysia;* [2]*Centre for Biomolecular Sciences, School of Pharmacy, University of Nottingham, Nottingham, UK;* [3]*Faculty of Agriculture, Universiti Putra Malaysia, Serdang, Selangor, Malaysia;* [4]*Faculty of Applied Sciences, University Technology MARA, Shah Alam, Selangor, Malaysia and* [5]*Laboratory of Natural Products, Institute of Bioscience, Universiti Putra Malaysia, Serdang, Selangor, Malaysia*

Background and purpose: Andrographolide, the major phytoconstituent of *Andrographis paniculata,* was previously shown by us to have activity against breast cancer. This led to synthesis of new andrographolide analogues to find compounds with better activity than the parent compound. Selected benzylidene derivatives were investigated for their mechanisms of action by studying their effects on the cell cycle progression and cell death.
Experimental approach: Microculture tetrazolium, 3-(4,5-dimethylthiazol-2-yl)-2,5-diphenyl tetrazolium bromide (MTT) and sulphorhodamine B (SRB) assays were utilized in assessing the *in vitro* growth inhibition and cytotoxicity of compounds. Flow cytometry was used to analyse the cell cycle distribution of control and treated cells. CDK1 and CDK4 levels were determined by western blotting. Apoptotic cell death was assessed by fluorescence microscopy and flow cytometry.
Key results: Compounds, in nanomolar to micromolar concentrations, exhibited growth inhibition and cytotoxicity in MCF-7 (breast) and HCT-116 (colon) cancer cells. In the NCI screen, 3,19-(2-bromobenzylidene) andrographolide (SRJ09) and 3,19-(3-chloro-4-fluorobenzylidene) andrographolide (SRJ23) showed greater cytotoxic potency and selectivity than andrographolide. SRJ09 and SRJ23 induced G_1 arrest and apoptosis in MCF-7 and HCT-116 cells, respectively. SRJ09 downregulated CDK4 but not CDK1 level in MCF-7 cells. Apoptosis induced by SRJ09 and SRJ23 in HCT-116 cells was confirmed by annexin V-FITC/PI flow cytometry analysis.
Conclusion and implications: The new benzylidene derivatives of andrographolide are potential anticancer agents. SRJ09 emerged as the lead compound in this study, exhibiting anticancer activity by downregulating CDK4 to promote a G_1 phase cell cycle arrest, coupled with induction of apoptosis.
British Journal of Pharmacology (2008) **155,** 641–654; doi:10.1038/bjp.2008.368; published online 22 September 2008

Keywords: andrographolide derivatives; antitumour; cell cycle; G_1 arrest; NCI cell lines; CDK-4; apoptosis; v-Src

Abbreviations: APS, ammonium persulphate; CDK, cyclin-dependent kinase; DMSO, dimethylsulphoxide; ECL, enzyme chemiluminescence; FCS, foetal calf serum; FITC, fluorescein isothiocyanate; HRP, horseradish peroxidase; MG_MID, mean graph midpoint; MTT, 3-(4,5-dimethylthiazol-2-yl)-2,5-diphenyl tetrazolium bromide; NSCL, non-small cell lung; PBS, phosphate-buffered saline; PI, propidium Iodide; PS, phosphatidylserine; PVDF, polyvinylidene fluoride; SDS, sodium dodecyl sulphate; SOM, self organizing map; SRB, sulphorhodamine B; TEMED, N,N,N′,N′-tetramethylethylenediamine

Introduction

The ethnomedicinal use of plants has had a very significant function in the development of formularies and pharmacopoeias, providing a major focus in global health care, as well as contributing substantially to the drug discovery and development process. Screening natural products obtained from plants, marine organisms, microorganisms and animals have yielded many pharmaceutical agents.

There are about 500 000 species of plants worldwide and it is estimated that at least 5000 different chemical compounds of secondary metabolites are present in a single species of plant (Verpoorte, 1998). It is clear that the secondary metabolites of plant origin constitute a vast source of new

Correspondence: Associate Professor Dr J Stanslas, Department of Biomedical Sciences, Faculty of Medicine and Health Sciences, Universiti Putra Malaysia, 43400 Serdang, Selangor, Malaysia.
E-mails: rcxjs@medic.upm.edu.my or jstanslas@yahoo.co.uk
[6]Current address: Department of Paediatrics, Laboratory of Human Genetics, Yong Loo Lin School of Medicine, National University of Singapore, Singapore.
Received 2 May 2008; revised 7 July 2008; accepted 11 August 2008; published online 22 September 2008

and useful drugs. Anticancer drugs, such as the semi-synthetic paclitaxel and docetaxel, arise from chemical modifications of a precursor obtained from *Taxus baccata* and are used to treat refractory ovarian, breast and other cancers. Topotecan and irinotecan, analogues of camptothecin, a natural product isolated from *Camptotheca acuminata* have made striking improvements in the treatment outcome of refractory ovarian, cervical, non-small cell lung and colon cancers. Podophyllotoxin from *Podophyllum peltatum*, synthetically modified into etoposide is used in the treatment of lung and testicular cancers. Other promising naturally occurring molecules include vinca alkaloids (vincristine and vinblastine), colchicines, ellipticine and flavopiridol (Mukherjee *et al*., 2001).

Andrographis paniculata Nees (Acanthaceae) is one of the most important medicinal plants, having been used in Ayurvedic medicine (a form of alternative medicine that is the traditional system of medicine of India) for gastric disorders, cold, influenza and other infectious diseases (Chakravarti and Chakravarti, 1952; Bensky and Gamble, 1993). Its common name is 'King of Bitters'. Extracts of the whole plant and the main phytoconstituent andrographolide (Figure 1) exhibit several pharmacological activities, including anti-inflammatory, immunostimulatory, antiviral, hypoglycemic, hypotensive, cytotoxicity and cardioprotective actions (Siripong *et al*., 1992; Puri *et al*., 1993; Matsuda *et al*., 1994; Chiou *et al*., 1998; Basak *et al*., 1999; Zhang and Tan, 2000a, b; Shen *et al*., 2002; Woo *et al*., 2008). Of all the properties mentioned above, the anti-inflammatory property of andrographolide has been extensively documented (Chiou *et al*., 1998; Shen *et al*., 2002; Wang *et al*., 2004) and the molecular mechanisms behind this effect have been elucidated by various groups (Chiou *et al*., 2000; Tsai *et al*., 2004; Xia *et al*., 2004; Hidalgo *et al*., 2005).

However, our interests have been focused more on the compound's anticancer potential. Andrographolide was reported by others and us to have antitumour activities in breast and colon cancer models (Stanslas *et al*., 2001; Rajagopal *et al*., 2003). Many studies have shown that andrographolide is a potent inducer of apoptosis in various cancer cell lines (Cheung *et al*., 2005; Zhou *et al*., 2006), substantiating its potential in cancer therapy. This compound also has the ability to induce G_1 cell cycle arrest through induction of p27 and suppression of cyclin-dependent kinase (CDK) 4 in human tumour cell lines (Rajagopal *et al*., 2003). The most intriguing finding on the mechanism of antitumour activity of andrographolide came from a recent study by Liang *et al*. (2008), who revealed this compound had a novel mechanism through its ability to promote degradation of the oncoprotein v-Src through attenuation of the Erk1/2-signalling pathway.

The many reports on the pharmacological properties of andrographolide, especially on its anticancer activity, prompted us to synthesize some derivatives and to evaluate their anticancer potential. The derivatives of andrographolide were synthesized by coupling of two hydroxyl groups at C-3 and C-19 (Figure 1) and was carried out by reacting andrographolide with different types of substituted aromatic aldehydes. A preliminary study to assess the cytotoxic effect of the resulting andrographolide derivatives has been carried out against the MCF-7 (breast) and HCT-116 (colon) cancer cell lines (Jada *et al*., 2006).

In this paper, we describe the anticancer properties of three benzylidene derivatives of andrographolide namely 3,19-(2-bromobenzylidene) andrographolide (SRJ09), 3,19-(3-bromobenzylidene) andrographolide (SRJ10) and 3,19-(3-chloro-4-fluorobenzylidene) andrographolide (SRJ23) (Figure 1), selected because they showed interesting *in vitro* anticancer profiles based on the National Cancer Institute (NCI) 60-cell line screen. We have elaborated extensively the *in vitro* anticancer activity of the compounds with particular emphasis on their cancer type selectivity. We also examined the effects of the compounds on the cell cycle progression and induction of apoptosis. In attempting to elucidate the mechanisms of cytotoxic activities of SRJ09 and SRJ23, we characterized some of the biochemical and molecular events occurring in the various stages leading to cell cycle arrest and cell death.

Materials and methods

Cell lines and cell culture

For routine testing, two types of cancer cell lines were used in this study: MCF-7 (human breast cancer) and HCT-116 (human colon cancer), which were purchased from the American Type Culture Collection (Manassas, VA, USA). For

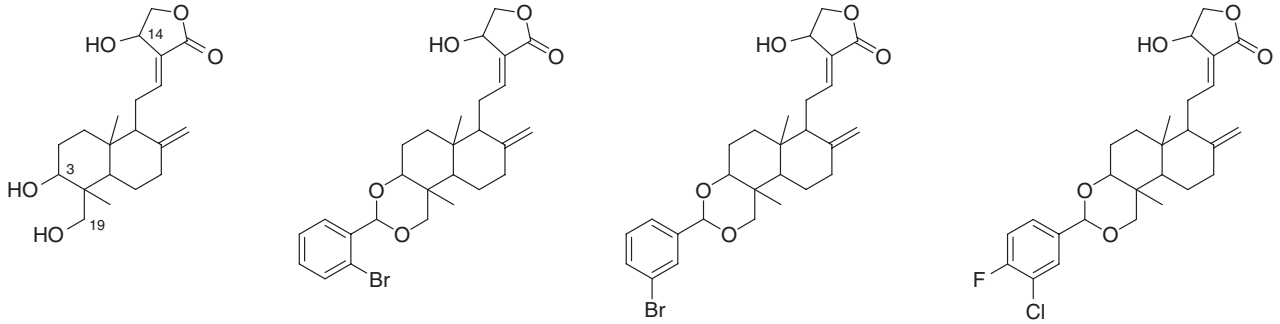

Andrographolide SRJ09 SRJ10 SRJ23

Figure 1 Structures of andrographolide and the three derivatives tested here.

the NCI screen, approximately 60 NCI human cancer cell lines representing cancer cells of leukaemia, non-small cell lung, colon, CNS, melanoma, ovarian, renal, prostate and breast were used to determine tumour type selectivity of compounds. Cells were maintained in RPMI-1640 medium with L-glutamine, supplemented with 10% heat inactivated (55 °C for 1 h) FCS, at 37 °C in an atmosphere of 5% CO_2 and 95% air.

Cell viability assays

MTT cell viability assay. The assay was carried out based on the method described by Mosmann (1983). Briefly, cells were plated in 96-well flat-bottomed tissue culture plates with 3000–5000 cells per well in 180 μL culture media. This was followed by incubation at 37 °C (5% CO_2 and 95% air) overnight to allow cell attachment on to the wells. The stock concentrations (100 mM) of test agents were made up in dimethylsulphoxide (DMSO). The working concentration ranging from 1 to 1000 μM was obtained by serial dilution in culture medium and 20 μL of each of the concentration was added into the appropriate wells in four replicates to obtain final concentrations ranging from 0.1 to 100 μM. The control cells were treated with the highest concentration of DMSO (0.1%) as vehicle control. Following a further 72 h incubation, 50 μL microculture tetrazolium, 3-(4,5-dimethylthiazol-2-yl)-2,5-diphenyl tetrazolium bromide (MTT) (2 mg mL^{-1} in PBS) was added per well and the plate was incubated for 4 h to allow metabolism of MTT by cellular mitochondrial dehydrogenases. The excess MTT was aspirated and the formazan crystals formed were dissolved by the addition of 150 μL of DMSO: glycine buffer (0.1 M glycine/0.1 M NaCl/pH 10.5) (4:1). The absorbance of purple formazan, proportional to the number of viable cells, was read at 550 nm using a microplate reader (Anthos Labtec Instruments GmbH, Salzburg, Austria). The results were analysed using Deltasoft 3 computer program (BioMetallics Inc., Princeton, NJ, USA). Using 0 and 72 h MTT absorbance values, the semilog dose–response curves (percentage of growth vs concentration) were constructed, from which the GI_{50} (concentration that produces 50% growth inhibition), TGI (concentration that produces total growth inhibition or cytostatic effect) and LC_{50} (−50% growth: lethal concentration or 'net cell killing' or cytotoxicity parameter) were determined.

Sulphorhodamine B assay. The SRB assay was used for assessing the growth inhibitory and cytotoxicity potential of test agents in a panel of cell lines representing nine different cancer types (Boyd and Paull, 1995). The assay was performed and cytotoxic activity was analysed at NCI, Bethesda, MD, USA.

Cell cycle analysis

Control and treated floating and adherent cells were collected by trypsinization and pelleted at 100 *g* for 5 min. Cells were washed two times with PBS and cells were resuspended in fluorochrome solution (0.1% sodium citrate, 0.1% Triton X-100, 50 μg mL^{-1} propidium iodide and 0.1 mg mL^{-1} RNAse) and incubated at 4 °C overnight. The DNA content of 20 000 cells for each determination was measured using Beckman Coulter EPICS-XL MCL flow cytometer (Beckman Coulter Inc., Fullerton, CA, USA) in which an argon laser (488 nm) was used to excite propidium iodide (PI) and emission above 550 nm was collected (Ormerod, 1999). Percentage of cells at various phases of the cell cycle was analysed using the computer advanced DNA cell cycle analysis software Multicycle for Windows (Phoenix Flow Systems, San Diego, CA, USA).

Western blot analysis

Exponentially growing cells (50% confluency) were treated with 1 and 7 μM of SRJ09 for 72 h. Treated cells were trypsinized, diluted in PBS, syringed and then pelleted by centrifugation at 100 *g* for 5 min. The cell pellet was then resuspended in lysis buffer (20 mM Tris-HCl pH 7.4, 2 mM EDTA pH 7.4, 2 mM EGTA pH 7.4, 6 mM β-mercaptoethanol, 10 μg mL^{-1} of leupeptin, 2 μg mL^{-1} of aprotinin and 1% Nonidet (NP-40)) and sonicated (Soniprep 150, MSE, USA) at 26 amplitude microns on ice. The cell lysate was centrifuged at 140 000 *g* for 15 min at 4 °C and the supernatant was collected and stored at −70 °C. The concentration of protein was determined using Bio-Rad protein assay reagent, according to the manufacturer's instructions. An equal amount of protein (50 μg) was separated by 10% SDS-PAGE. After electrophoresis, the proteins were transferred to PVDF membrane, blocked overnight with 1% skimmed milk in TBS at 4 °C, reacted with mouse monoclonal antibody against CDK1, CDK4 or Actin (Ab-1) and washed. After reaction with horseradish peroxidase-conjugated goat anti-mouse antibody, the immune complexes were visualized by using the ECL-detection reagents following the manufacturer's procedure.

Detection of cell death

Morphological changes. Control and treated adherent and floating cells were collected and washed three times in cold PBS. After every wash the cells were pelleted by centrifugation (100 *g* for 5 min at room temperature). 100 μL of 10 μg mL^{-1} acridine orange was added to the cell pellet and incubated for 10 min on ice. Here, 50 μL of the cell suspension was visualized immediately under blue light excitation (485 nm) of Leitz Dialux 20 fluorescence microscope, which exhibits DNA as yellow, RNA as red and cytoplasm as green. Fluorescence micrographs were captured using a Nikon Coolpix 4500 camera (Tokyo, Japan).

Annexin V-FITC and propidium iodide double staining analysis by flow cytometry: detection of externalized phosphatidylserine (PS). Cells were plated at appropriate densities (approximately 2.5×10^4 cells per well) in 3 mL of medium in 6-well plates (Nalge-Nunc, Rochester, NY, USA). Following the desired treatment period, the floating cells were collected and the adherent cells were trypsinized. Both floating and adherent cells were washed in medium, centrifuged and then resuspended in 2 mL of medium. Cells were counted and a volume of media containing 1×10^5 cells was centrifuged to obtain a pellet. After dislodging the pellet, 100 μL of 1 ×

assay buffer and 5 μL of annexin V-fluorescein isothiocyanate (FITC) were added and the sample was mixed by gentle tapping. Following 20 min incubation at room temperature in the dark, 400 μL of 1 × assay buffer and 10 μL of PI (50 μg mL^{-1}) were added and the samples were analysed immediately using Beckman Coulter EPICS-XL MCL flow cytometer (Beckman Coulter Inc., USA). The green fluorescence (FITC) and red fluorescence (PI) were detected by filtration through 530 and 585 nm band pass filters, respectively. For each sample, 10 000 events were collected.

Statistical analysis

Statistical comparisons were made using one-way ANOVA (more than one group) by Statistical Package for Social Sciences (SPSS) version 10.00. The differences were considered statistically significant if $P<0.05$.

Materials

All the andrographolide analogues were synthesized in our laboratory (Jada *et al*., 2006). Acridine orange, ammonium persulphate, bovine serum albumin, bromophenol blue, DMSO, *N*,*N*,*N*′,*N*′-tetramethylethylenediamine (TEMED), polyoxyethylene sorbitan monolaurate (Tween 20), PI, MTT, ethyleneglycol-bis-(β-amino ethylether)-*N*,*N*,*N*′,*N*′-tetraacetic acid (EGTA), glycerol, leupeptin, 2-mercaptoethanol, *N*,*N*′-methylene-bis-acrylamide, sodium dodecyl sulphate (SDS), SRB, Tris-base, Triton X-100 and trypsin-ethylenediaminetetra-acetic acid disodium salt (EDTA) were purchased from Sigma (Poole, UK). Glycine, sodium chloride, sodium hydroxide and hydrochloric acid were supplied by Fisher Scientific (Loughborough, UK). EDTA and Tris(hydroxymethyl)methylamine (Tris) were purchased from BDH Chemicals Ltd (Poole, UK). BioRad protein assay reagent was purchased from Bio-Rad Laboratories Ltd (Hemel Hempstead, UK). Enzyme chemiluminescence (ECL) reagents, polyvinylidene fluoride (PVDF) and hyperfilm ECL were supplied by Amersham International plc (Aylesbury, UK). RNase A was purchased from Boehringer Mannheim UK Ltd (Lewes, UK). Phosphate-buffered saline (PBS) tablets were obtained from Oxoid Laboratories Ltd (Hampshire, UK). Horseradish peroxidase-conjugated goat anti-mouse antibody was purchased from Pierce (Chester, UK). Mouse monoclonal antibodies against CDK1 and CDK4, and Actin (Ab-1) were obtained from BD Biosciences (CA, USA) and Oncogene Research Products (CA, USA), respectively. RPMI-1640 medium with L-glutamine, penicillin–streptomycin, trypsin-EDTA, tissue culture flasks and multi-well plates were purchased from Life Technologies (Paisley, UK). Foetal calf serum (FCS) was obtained from Globepharm (Escher, UK). Annexin-V apoptosis detection kit was purchased from Santa Cruz Biotechnology (CA, USA) and it contained Annexin-V-FITC (50 μg in 250 μL buffer), 10 × assay buffer and propidium iodide (50 μg mL^{-1} solution PBS).

Results

Growth inhibitory properties of andrographolide derivatives in pre-screen and 60 NCI cancer cell lines

Andrographolide, SRJ09, SRJ10 and SRJ23 were first evaluated for anticancer activity in MCF-7 and HCT-116 cancer cell lines. In the conventional tetrazolium-based assay, SRJ09, SRJ10 and SRJ23 were found to be almost equally potent as the parent compound in inhibiting the growth of both cell lines, based on GI_{50} values (Table 1). However, SRJ09, SRJ10 and SRJ23 caused significantly higher ($P<0.05$) cytostatic (TGI values) and cytocidal (LC_{50} values) effects in MCF-7 cells, compared with the parent compound. A similar effect was observed in HCT-116 cells at LC_{50} level but not at TGI level, whereby the cytostatic effect of the tested compounds were similar.

In the NCI screen, the SRB end point assay was used to calculate the GI_{50}, TGI and LC_{50} dose–response growth inhibitory parameters (Boyd and Paull, 1995). In addition, a mean graph midpoint (MG_MID) was calculated for each of the parameter giving an averaged activity parameter over all the cell lines (Table 2). For the calculation of the MG_MID, insensitive cell lines are included with the highest concentration tested. For identification of cytotoxic potency and selectivity of test agents, GI_{50} values less than 1 μM were considered to have significant activity. From Table 2, SRJ09 was effective against leukaemia (RPMI-8226), colon (SW-620), CNS (U251) and melanoma (LOX IMVI); SRJ23 was effective against leukaemia (CCRF-CEM), NSCL (HOP-92) and prostate (PC3); SRJ10 was not effective against any type of cell lines; the parent compound andrographolide was effective only in one cell line, HT-29 colon cancer. Interestingly, although some of the compounds had low GI_{50} values, they displayed higher LC_{50} values (>100 μM): SRJ09 in RPMI-8266 and SW-620, SRJ23 in CCRF-CEM. By

Table 1 Dose–response growth inhibitory parameters of andrographolide and its derivatives in *in vitro* anti-cancer pre-screen cell lines

Compounds	*GI_{50}*		*TGI*		*LC_{50}*	
	MCF-7	*HCT-116*	*MCF-7*	*HCT-116*	*MCF-7*	*HCT-116*
Andrographolide	6.4 ± 2.1	5.1 ± 0.1	64.7 ± 12.2	15.5 ± 9.3	81.1 ± 17.5	39.5 ± 9.1
SRJ09	4.2 ± 2.8	3.8 ± 3.5	8.8 ± 1.1	8.1 ± 1.6	9.4 ± 0.3	8.6 ± 1.2
SRJ10	5.3 ± 1.6	4.7 ± 0.3	43.2 ± 3.1	9.0 ± 0.5	56.6 ± 4.4	9.6 ± 1.1
SRJ23	5.2 ± 1.8	3.8 ± 1.7	9.1 ± 1.5	8.7 ± 0.2	9.5 ± 0.3	9.4 ± 0.1

The pre-screen cell lines used here were: human breast (MCF-7) cancer and colon (HCT-116) cancer cells. The cells were treated for 72 h with at least four different concentrations of compounds ranging from 0.1 to 100 μM. MTT assay (Mosmann, 1983) was used to calculate GI_{50}, TGI and LC_{50} values (expressed in μM). Values are mean of at least three separate experiments and errors represent the s.d. values.

Table 2 Inhibition of *in vitro* cancer cell lines by andrographolide, SRJ09 (NSC729655), SRJ10 (NSC732585) and SRJ23 (NSC732589)

Panel cell line	*Andrographolide*			*SRJ09*			*SRJ10*			*SRJ23*		
	GI_{50}	*TGI*	LC_{50}	GI_{50}	*TGI*	LC_{50}	GI_{50}	*TGI*	LC_{50}	GI_{50}	*TGI*	LC_{50}
Leukaemia												
HL-60(TB)	15.84	100	100	4.89	>100	>100	NT	NT	NT	2.13	>100	>100
CCRF-CEM	3.98	100	100	NT	NT	NT	24.54	>100	>100	**0.37**	5.37	>100
K-562	3.16	100	100	6.16	>100	>100	5.24	19.05	72.44	2.34	6.02	51.28
MOLT-4	25.11	100	100	>100	>100	>100	NT	NT	NT	2.63	>100	>100
RPMI-8226	5.01	50.11	100	**0.29**	6.30	>100	NT	NT	NT	NT	NT	NT
Non-small cell lung cancer												
A549/ATCC	25.11	39.81	100	8.91	>100	>100	3.63	15.48	87.09	2.51	7.58	>100
EKVX	31.62	100	100	18.19	40.73	89.12	22.90	45.70	91.20	15.13	34.67	79.43
HOP-62	31.62	50.11	100	>100	>100	>100	14.45	28.84	57.54	15.13	29.51	57.54
HOP-92	25.11	63.09	100	11.48	29.51	74.13	20.89	44.66	95.49	**0.17**	1.58	6.91
NCI-H226	39.81	100	100	NT	NT	NT	3.16	>100	>100	1.94	3.38	5.88
NCI-H23	19.95	50.11	100	14.45	42.65	>100	9.12	24.54	63.09	6.59	33.11	66.06
NCI-H322M	31.62	100	100	NT	NT	NT	15.84	32.35	66.06	5.62	19.05	46.77
NCI-H460	19.95	63.09	100	10.00	39.81	>100	3.01	10.71	41.68	12.02	45.70	>100
NCI-H522	10.00	25.11	79.43	4.36	38.90	>100	4.67	28.84	>100	4.26	32.35	>100
Colon cancer												
COLO 205	15.84	15.84	50.11	7.58	52.48	>100	20.89	35.48	60.25	1.90	3.89	7.94
HCC-2998	25.11	50.11	100	NT	NT	NT	4.16	15.48	54.95	16.21	31.62	61.65
HCT-116	15.84	31.62	63.09	1.58	>100	>100	1.99	3.89	7.76	2.45	5.12	12.58
HCT-15	15.84	39.81	100	2.18	12.02	69.18	13.48	>100	>100	11.22	33.11	97.72
HT29	**0.50**	25.11	100	5.24	>100	>100	5.12	30.19	>100	2.39	7.76	50.11
KM12	15.84	25.11	50.11	18.19	64.56	>100	5.24	19.95	67.60	2.34	11.48	46.77
SW-620	10.00	25.11	63.09	**0.45**	30.19	>100	5.24	26.91	>100	3.63	12.88	>100
CNS cancer												
SF-268	25.11	100	100	15.13	35.48	83.17	4.36	16.98	46.77	17.37	42.65	>100
SF-295	19.95	50.11	100	NT	NT	NT	20.89	43.65	91.20	2.23	10.71	43.65
SF-539	19.95	39.81	100	7.41	25.11	79.43	7.07	26.30	91.20	2.75	5.01	9.12
SNB-19	50.11	100	100	14.45	38.01	>100	18.62	32.35	57.54	3.16	9.12	41.68
SNB-75	15.84	31.62	63.09	14.79	>100	>100	15.84	38.01	89.12	1.90	4.78	48.97
U251	10.00	25.11	50.11	**0.29**	0.933	4.36	3.16	13.80	60.25	7.94	24.54	70.79
Melanoma												
LOX IMVI	12.58	100	79.43	**0.44**	1.69	4.57	2.95	5.49	>100	4.07	14.79	43.65
M14	15.84	31.62	100	NT	NT	NT	5.13	19.49	72.44	7.07	22.38	64.56
SK-MEL-2	15.58	31.62	63.09	11.22	>100	>100	9.33	>100	>100	2.58	79.43	>100
SK-MEL-28	15.84	25.11	50.11	2.63	18.19	>100	19.49	36.30	69.18	2.13	4.67	10.00
SK-MEL-5	19.95	25.11	50.11	12.30	27.54	61.65	17.37	32.35	61.65	13.48	28.18	60.25
UACC-257	19.95	39.81	100	20.41	48.97	>100	3.71	8.91	42.65	2.08	4.36	9.12
UACC-62	19.95	63.09	100	10.47	22.90	51.28	5.75	22.38	67.60	2.04	3.98	7.76
Ovarian cancer												
IGROV1	19.95	63.09	100	NT	NT	NT	7.24	30.90	>100	8.31	93.32	>100
OVCAR-3	10.00	19.95	50.11	9.54	26.91	72.44	21.87	42.65	83.17	1.31	3.98	38.01
OVCAR-4	10.00	25.11	50.11	NT	NT	NT	NT	NT	NT	2.13	4.57	9.77
OVCAR-5	15.84	25.11	63.09	23.44	93.32	>100	12.58	29.51	69.18	16.98	36.30	75.85
OVCAR-8	10.00	25.11	50.11	2.34	>100	>100	1.77	4.67	38.01	2.23	4.46	9.12
SK-OV-3	25.11	63.09	100	10.00	63.09	>100	18.19	32.35	56.23	14.79	28.84	56.23
Renal cancer												
786-0	5.01	19.95	39.81	1.81	>100	>100	3.46	12.02	48.97	4.57	16.21	47.86
A498	31.62	100	100	25.70	56.23	>100	25.70	47.86	89.12	18.19	39.81	89.12
ACHN	31.62	100	100	1.28	2.69	5.49	14.79	36.30	87.09	16.21	33.11	66.06
RXF 393	19.95	31.62	63.09	16.59	33.11	67.60	NT	NT	NT	3.71	>100	>100
CAKI-1	NT	NT	NT	11.48	57.54	>100	26.91	64.56	>100	1.73	4.07	9.54
SN12C	15.84	39.81	79.43	1.73	7.24	33.88	3.89	23.98	>100	2.08	3.98	7.41
TK-10	50.14	100	100	26.3	61.65	>100	11.74	33.88	100	3.54	14.45	41.68
UO-31	39.81	100	100	1.81	7.07	>100	12.58	34.67	95.49	16.98	60.25	>100
Prostate cancer												
PC-3	19.95	79.43	100	10.00	27.54	74.13	14.79	30.19	63.09	**0.4**	1.65	7.07
DU-145	39.81	100	63.09	15.48	34.67	79.43	16.59	31.62	61.65	3.31	10.47	47.86

Table 2 *Continued*

Panel cell line	*Andrographolide*			*SRJ09*			*SRJ10*			*SRJ23*		
	GI_{50}	*TGI*	LC_{50}	GI_{50}	*TGI*	LC_{50}	GI_{50}	*TGI*	LC_{50}	GI_{50}	*TGI*	LC_{50}
Breast cancer												
MCF-7	15.84	31.62	100	1.23	>100	>100	1.77	4.26	11.74	5.75	>100	>100
NCI/ADR-RES	25.11	100	100	3.46	>100	>100	5.24	36.30	>100	13.18	32.35	77.62
MDA-MB-231/ATCC	25.11	63.09	50.11	1.58	5.24	42.65	3.71	>100	>100	1.94	3.63	6.91
HS 578T	39.81	100	100	22.90	81.28	>100	38.01	100	>100	28.84	>100	>100
MDA-MB-435	10.00	25.11	50.11	4.16	23.44	>100	18.19	38.01	77.62	1.69	3.63	7.76
BT-549	2.94	19.95	50.11	NT	NT	NT	6.76	38.01	>100	4.36	9.77	75.85
T-47D	25.11	39.81	100	12.02	97.72	>100	19.49	35.48	64.56	1.51	3.54	8.12
MG_MID	20.30	56.95	83.41	6.02	16.98	77.62	8.01	28.18	70.79	4.07	12.88	38.01

Data shown in the Table were obtained from the NCI's *in vitro* disease-oriented human tumour cells screen (Boyd and Paull, 1995). Values are expressed in μM. NT: not tested.

In the last row of the Table, mean panel values or mean graph midpoints (MG_MID) are shown. These values of the response parameters were obtained by averaging the individual values for each cell line. If the indicated effect was not attainable within the used concentration interval, the highest concentration was used for the calculation.

Values in bold indicate $GI_{50} < 1$ μM.

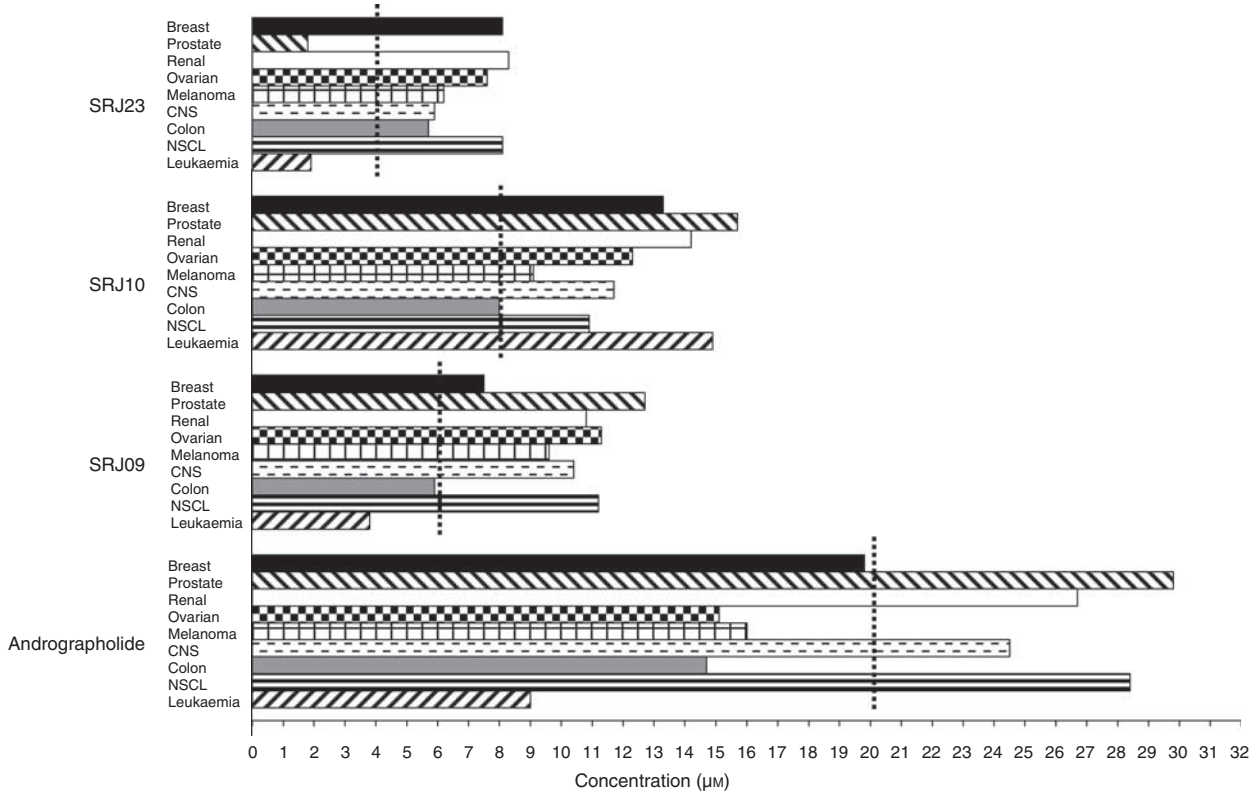

Figure 2 Mean growth inhibitory concentration (GI_{50}) of SRJ09, SRJ10 and SRJ23 compared with andrographolide in a subset of cells in the NCI *in vitro* anticancer screen. Andrographolide was selective towards leukaemia and non-selective against prostate; SRJ09 was selective towards leukaemia and non-selective against prostate cancer; SRJ10 was selective towards colon cancer and non-selective against prostate cancer; SRJ23 was selective towards prostate cancer and renal cancer. The vertical lines are the overall mean GI_{50} values across all cancer cell lines for each of the compound. SRJ09, SRJ10 and SRJ23 were relatively more potent than andrographolide against all cancer types. The values for andrographolide are based on previous screens conducted by the NCI, where the highest concentration tested was also 100 μM.

comparing the MG_MID values for the three parameters, the potencies of the compounds were ranked: GI_{50} and TGI, SRJ23 > SRJ09 > SRJ10 > andrographolide, LC_{50}, SRJ23 > SRJ10 > SRJ09 > andrographolide. Overall, the three semisynthetic compounds were more active than the parent compound.

By averaging the GI_{50} values of the cell lines representing each cancer type (Figure 2), it was found that andrographolide and SRJ09 were most active in leukaemia and least active in prostate cancer; SRJ10 was most active in colon cancer and least active in prostate cancer; SRJ23 was most active in prostate cancer and least active in renal cancer.

Inhibition of cell cycle progression

SRJ09 and SRJ10 induced a G_1 phase cell cycle arrest in MCF-7 cells at 24, 48 and 72 h time points when treated with 7 μM concentration with reduction in the number of cells in the S phase (Figure 3) and at times the G_1 arrest was accompanied with a concomitant decrease in both S and G_2/M phase cells. Induction of apoptosis by SRJ09 was demonstrated by the presence of a substantial number of cells in the sub-G1 population, in cells treated for 48 and 72 h. However, cells treated with SRJ10 did not show the presence of an apoptotic population. At 24, 48 and 72 h time points, 3 μM SRJ23 induced a G_1 phase block in HCT-116 cells (Figure 4). When the concentration of SRJ23 was increased to 6 μM, there was a dramatic increase in apoptotic cells at all the three time points.

Effect of SRJ09 on CDK1 and CDK4 protein levels in MCF-7 cells

From the cell cycle analysis, it was apparent that SRJ09 induced a G_1 phase block at all the three time points. To correlate this effect with the expression of proteins that control cell cycle progression namely CDK1 and CDK4, western blots were performed on protein lysates of MCF-7 cells treated with 1 and 7 μM of SRJ09 for 72 h. SRJ09 downregulated levels of CDK4 but did not affect CDK1 (Figure 5). These results strongly indicated that SRJ09 induced G_1 phase cell cycle arrest by downregulating CDK4 expression.

Morphological study of apoptosis

The effects of SRJ09 and SRJ23 were further analysed for their ability to induce apoptosis by the acridine orange fluorescence staining method. After treatment with SRJ09 and SRJ23 for 48 h, a high proportion of HCT-116 cells exhibited extensive nuclear condensation and fragmentation that are characteristics of apoptosis (Figure 6).

Annexin V-FITC/PI: flow cytometry analysis of apoptosis

For confirmation of apoptosis induced by SRJ09 and SRJ23, measurement of externalization of PS, an early event during

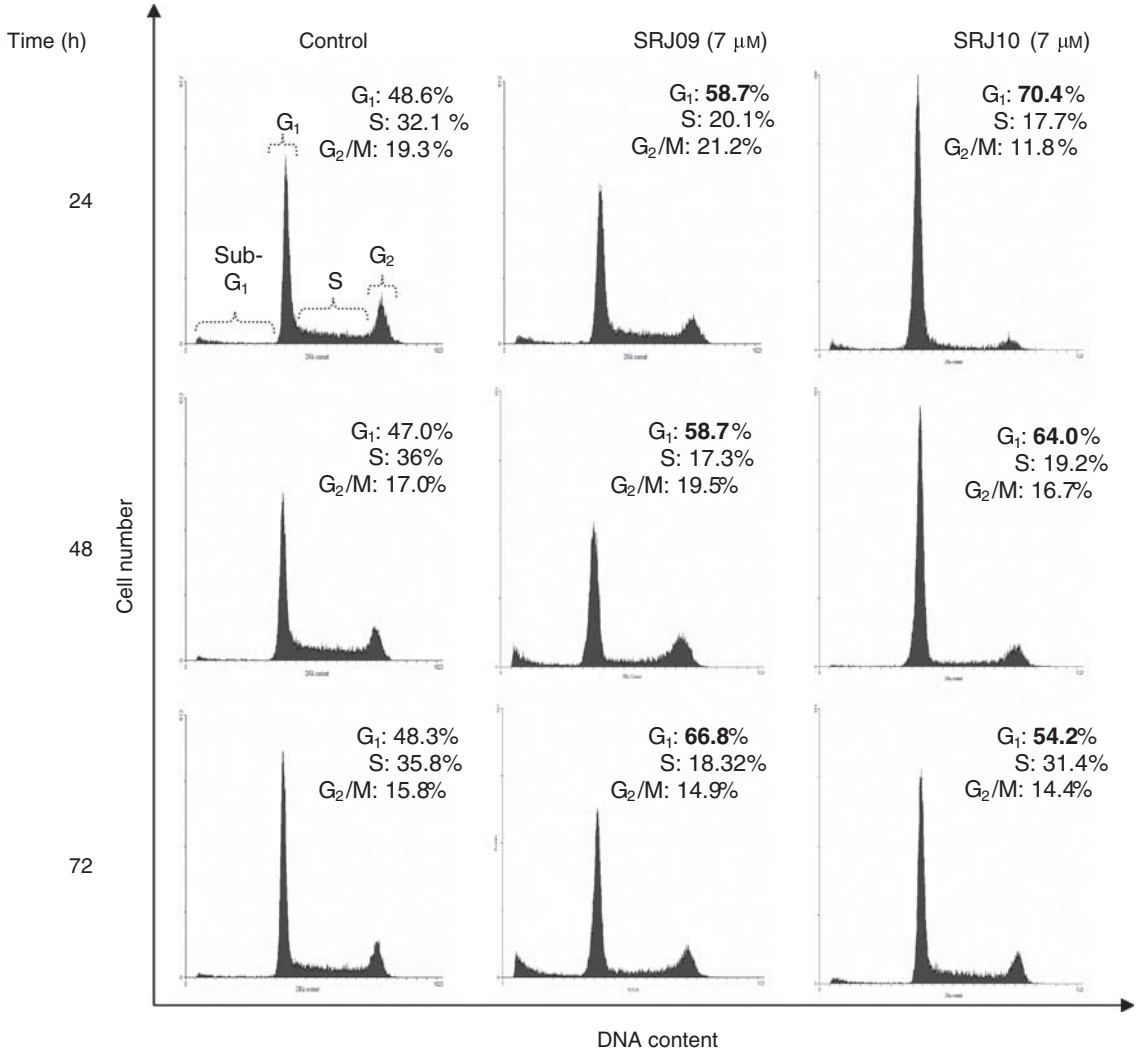

Figure 3 DNA histograms showing the cell cycle phase distribution of control, SRJ09- and SRJ10-treated MCF-7 cells. These figures are from representative experiments carried out at least two times. The *x* axis and *y* axis represent DNA content and cell number, respectively. Numbers in bold correspond to the significant variations compared to control.

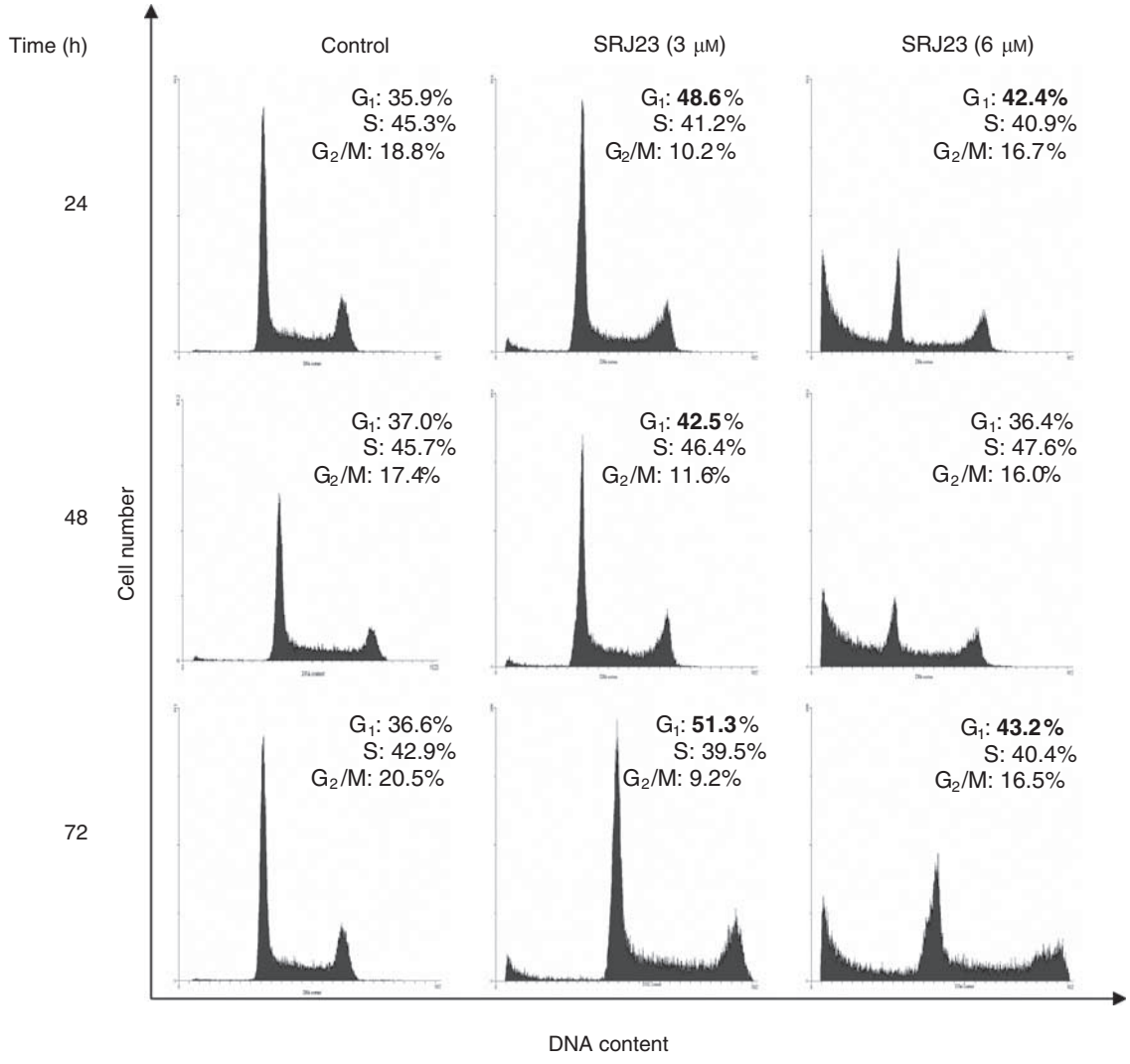

Figure 4 DNA histograms showing the cell cycle phase distribution of control and SRJ23-treated HCT-116 cells. These figures are from representative experiments carried out at least two times. The *x* axis and *y* axis represent DNA content and cell number, respectively. Numbers in bold correspond to the significant variations compared to control.

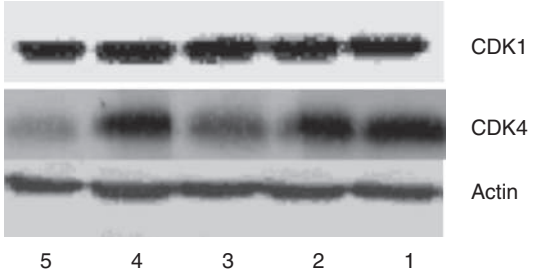

Figure 5 Western blot analysis of lysates from SRJ09-treated MCF-7 cells with CDK1, CDK4 and actin antibodies. The antiactin antibody was used to ensure equal amount of protein were loaded. Lane 1: control cells, medium alone without vehicle, Lane 2 and 4: cells treated with DMSO as vehicle, corresponds to amount of DMSO in 1 and 7 μM SRJ09 respectively, Lane 3 and 5: cells treated with 1 and 7 μM SRJ09, respectively.

apoptosis, by double staining with annexin V-FITC and PI was performed (Andree *et al*., 1990). The induction of apoptosis in HCT-116 cells treated with test agents was observed at 10, 24 and 48 h. Compared with that of the control, the number of live cells in drug-treated HCT-116 cells decreased dramatically with increasing concentrations at all the time points (Figures 7 and 8; Table 3). The reduction of live cells was time- and concentration-dependent in cells treated with SRJ09 and SRJ23. Similarly, the percentages of total apoptotic cells were significantly increased in a time- and concentration-dependent fashion in test agent-treated HCT-116 cells compared with control cells. Generally, more cells were in the late apoptotic phase with increased exposure time and concentration of compounds. This study confirms that apoptosis is the main mode of cell death induced by these two agents in HCT-116 cells.

Discussion and conclusions

Our search for local Malaysian medicinal plants with *in vitro* antitumour potential has led us to the identification of *A. paniculata* as a promising source of compounds with

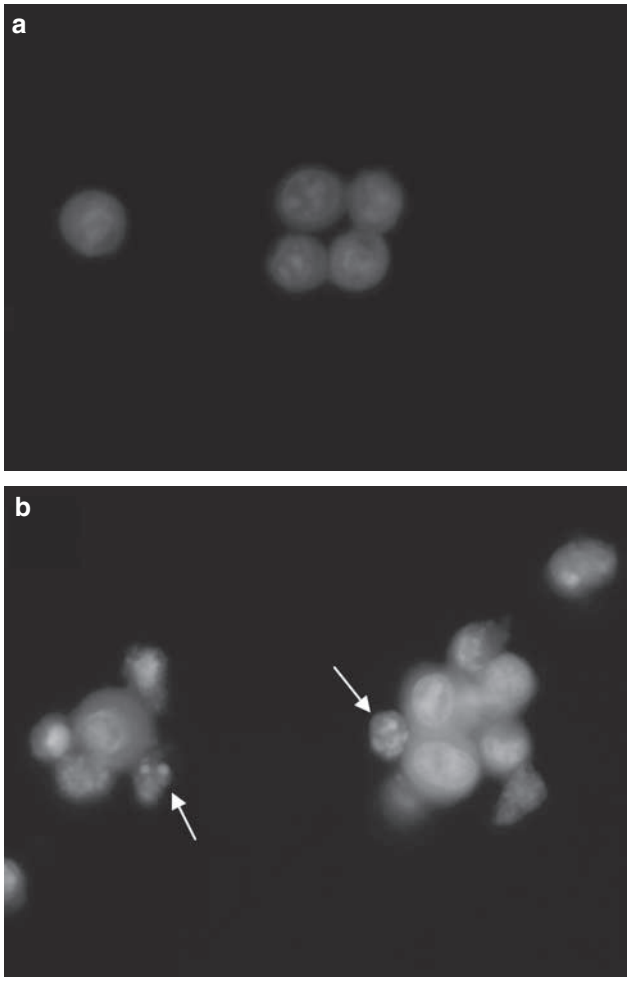

Figure 6 Acridine orange staining of floating and adherent (**a**) control and (**b**) 7 μM SRJ09-treated HCT-116 cells performed at 48 h. Compound-treated cells show nuclear condensation and fragmentation (indicated by arrow heads), features of apoptosis. Magnification, × 800.

impressive bioactivity *in vitro*. The main components of extracts *A. paniculata* are the diterpene lactones, of which, andrographolide is the major constituent. In a previous study, andrographolide was shown by us to possess *in vitro* and *in vivo* antitumour activities against human breast tumour models (Stanslas *et al*., 2001). This was followed by another report claiming the anticancer potential of andrographolide against colon cancer as evidenced by its cytotoxic and immunomodulating activities (Rajagopal *et al*., 2003). Based on the facts that andrographolide showed significant antitumour effects against breast and colon cancer models, and the ease of isolation of this compound in very good yield from *A. paniculata*, attempts were made to synthesize derivatives of andrographolide and examine their antitumour activities against different tumour cell lines (Jada *et al*., 2006, 2007).

In this study, the cytotoxic activities of andrographolide and its derivatives were first tested against MCF-7 and HCT-116 cancer cell lines. Andrographolide analogues caused a significant concentration-dependent reduction in proliferation and viability of both MCF-7 and HCT-116 cells. The compounds showed similar activities against both MCF-7 and HCT-116 cell lines as indicated by the GI_{50} values (Table 1). With respect to TGI and LC_{50} values, the derivatives overall showed better activity compared with that of the parent compound.

As the compounds had shown promising *in vitro* anticancer activity against the pre-screen cells, they were screened against the NCI panel of 60 tumour cell lines derived from nine different cancer types: leukaemia, melanoma, lung, colon, CNS, ovarian, renal, prostate and breast (Boyd and Paull, 1995). Testing of compounds against the NCI 60 cell line panel gives extensive information on the growth inhibitory effects of molecules across a wide variety of human tumour cell lines including cell type-specific effects (selective growth inhibition or cytotoxic properties) (Monks *et al*., 1991). For the analysis of activity of compounds in the NCI screen, a GI_{50} value of less than 1 μM was considered as an agent showing potency and potentially reflects selectivity towards that particular cancer cell line(s), hence such a compound could be considered to have therapeutic potential for the treatment of such types of cancer. SRJ09 was most active against leukaemia (RPMI-8226), melanoma (LOX IMVI), colon (SW-620) and CNS (U251) tumour cells, whereas SRJ23 was very active against leukaemia (CCRF-CEM), prostate (PC-3) and NSCL (HOP-92) cancers. However, SRJ10 failed to exhibit adequate potency. Andrographolide was most active against colon tumour cells (HT-29). By comparing the mean values of the three parameters of growth inhibition (GI_{50}, TGI and LC_{50}), we concluded the semisynthetic derivatives had improved *in vitro* cytotoxic activities compared with that of andrographolide. When the mean GI_{50} values of the different cancer types were taken into consideration (Figure 2), the compounds showed distinct patterns of activity: andrographolide and SRJ09 had similar activity, being most active against leukaemia and least activity towards prostate cancer; leukaemia cells were most responsive and prostate cancer cells were most resistant to SRJ10; SRJ23 had the most extreme difference in activity profile compared with others whereby it was most active against prostate and least active against renal cancer. This clearly indicates SRJ23 has potential in the treatment of prostate cancer.

Another benefit of the NCI screen is that it allows comparison to be made of the activity patterns of test agents with that of 171 standard anticancer agents of known mechanisms of action (Boyd, 1989). Using the *in silico* COMPARE (Weinstein *et al*., 1997) and SOM (Covell *et al*., 2003) analyses, the semisynthetic derivatives were found to have distinct mechanisms of action different from that of the standard anticancer agents (Jada *et al*., 2005), suggesting novel molecular targets for their anticancer activities. A recent finding further supports this suggestion as the parent compound andrographolide was shown to have novel mechanisms of antitumour activity by targeting the oncoprotein v-Src through attenuation of the Erk1/2 signalling pathway (Liang *et al*., 2008). This is indeed encouraging as SOM analysis of andrographolide revealed its mechanisms of action was different from that of standard anticancer agents and potentially novel (Jada *et al*., 2007). Therefore, it is

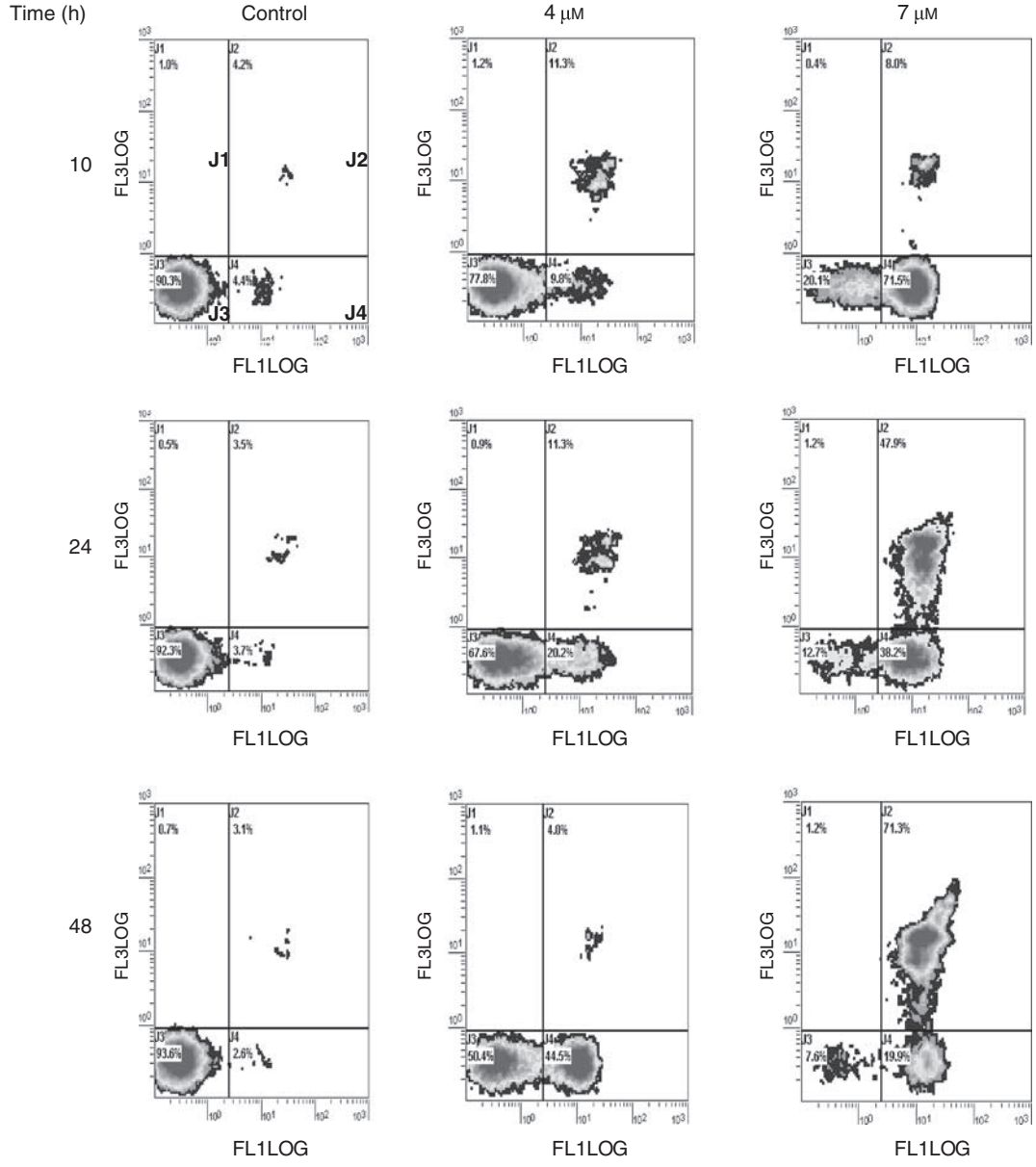

Figure 7 Density plots showing the percentage distribution of HCT-116 control and SRJ09 (10, 24 and 48 h) treated cells. Quadrants: (top left) J1—damaged cells, (top right) J2—late apoptotic/secondary necrotic cells, (lower left) J3—live cells, (lower right) J4—early apoptotic cells. These figures are from representative experiments carried out at least two times and mean values are presented in Table 3. FL1 = FITC fluorescence, FL3 = PI fluorescence.

highly possible that v-Src might be one of the molecular targets of SRJ09, as this compound was also projected in the same Q region in the SOM map as andrographolide, whereas SRJ23 was projected in the R region, another region without known mechanism(s) of action (Jada *et al*., 2005).

From the NCI screen, SRJ09 was selected as a lead compound because of its pronounced antitumour selectivity compared with other andrographolide derivatives (including the parent compound). To study the cellular and molecular mechanisms of action, SRJ09 and SRJ23 were selected for evaluation in MCF-7 and HCT-116 cells. For determination of cell cycle perturbations by the new agents, flow cytometric analysis was used to measure the DNA contents of SRJ09 and SRJ10 treated MCF-7 cells, and SRJ23-treated HCT-116 cells. Any change in the cell cycle progression will be reflected in the appearance of the DNA histogram produced. Hence, it is possible to study cell cycle arrest brought about by the cytotoxic agents. Following exposure time of 24, 48 and 72 h, SRJ09 and SRJ10 showed a specific G_1 phase cell cycle arrest in MCF-7 cells (Figure 3) unlike the parent compound which showed non-phase-specific cell cycle arrest (Jada *et al*., 2003). It is interesting to note although both SRJ09 and SRJ10 are isomers, SRJ09 induced apoptosis and more potent (in the NCI *in vitro* screen) than SRJ10, suggesting that changes in the position of the bromine substituent in the aromatic ring produces different biological

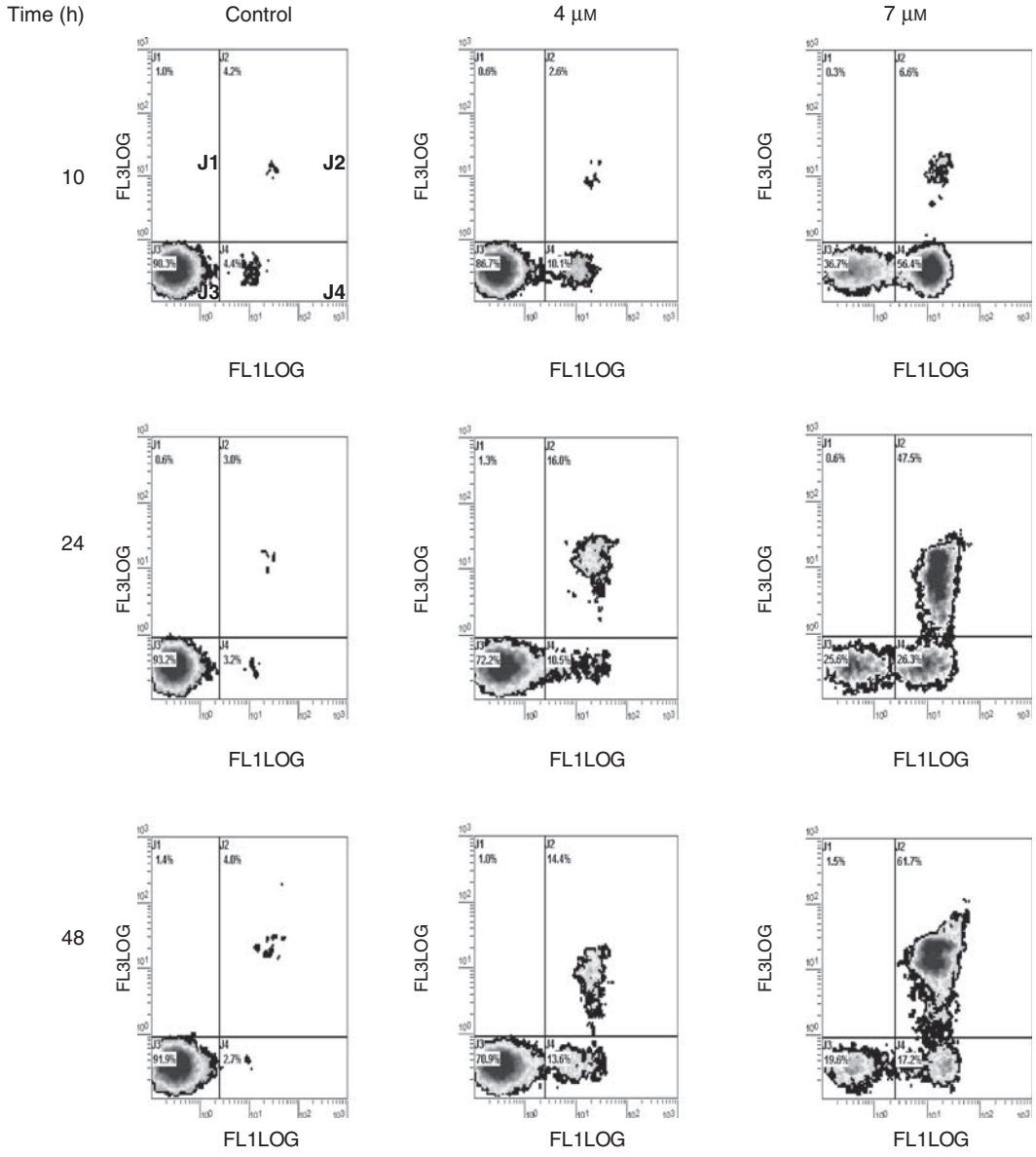

Figure 8 Density plots showing the percentage distribution of HCT-116 control and SRJ23 (10, 24 and 48 h) treated cells. Quadrants: J1—damaged cells, J2—late apoptotic/secondary necrotic cells, J3—live cells, J4—early apoptotic cells. These figures are from representative experiments carried out at least two times and mean values are presented in Table 3. FL1 = FITC fluorescence, FL3 = PI fluorescence.

sequelae. SRJ23-treated HCT-116 cells exhibited G_1 phase arrest and induction of sub-G_1 population, indicative of apoptotic cells (Figure 4). Thus, by the addition of a benzylidene pharmacophore at 3,19-positions to the andrographolide structure, it is possible to produce phase-specific cell cycle blocking agents and potent apoptosis inducers.

The CDKs are a group of serine/threonine kinases important in controlling the cell cycle in eukaryotic cells (Morgan, 1995). CDKs are responsible for phosphorylating various substrates critical to cell cycle progression (Piwnica-Worms, 1999; Sampath and Plunkett, 2001). Cyclins form heterodimeric complexes with specific CDKs at distinct points in the cell cycle to phosphorylate target proteins and promote cell cycle progression. CDK4 and CDK6 are thought to be involved in early G_1, CDK2 is required to complete G_1 and initiate S phase, and CDK1 regulates G_2/M phase (Hall and Peters, 1996; Bartek and Lukas, 2001). Two families of CDK inhibitors block the progression from G_1 to S phase by negatively regulating the kinase activity of different CDKs: the Cip/Kip and INK4 families (Harper and Elledge, 1996; Sherr and Roberts, 1999). The Cip/Kip family comprises $p21^{Cip1}$, $p27^{Kip1}$ and $p57^{Kip2}$ and INK4 family comprises $p16^{INK4a}$, $p15^{INK4b}$, $p18^{INK4c}$ and $p19^{INK4d}$. The Cip/Kip family shows broad kinase specificity whereas INK4 family members only bind and inhibit CDK4 and CDK6 (Brooks *et al*., 1998; Lee *et al*., 1999). Our investigation showed that the growth of MCF-7 cells was arrested in the G_1 phase of the cell cycle when treated with SRJ09. The effects of SRJ09 on the cell cycle progression was correlated with a specific biochemical expression of key cell cycle proteins

Table 3 Percentage of live, early apoptotic and late apoptotic/secondary necrotic cells in control and treated (SRJ09 and SRJ23) HCT-116 cells (see Figures 7 and 8 for typical results)

Compound	*Concentration (μM)*	*Time (h)*								
		10			*24*			*48*		
	Phase	*J2*	*J3*	*J4*	*J2*	*J3*	*J4*	*J2*	*J3*	*J4*
Control		3.6	91.1	4.1	3.9	91.5	4.3	3.5	93.2	2.3
SRJ09										
	4	10.4	77.9	11.0	11.9	64.3	22.9	4.9	49.6	44.8
	7	8.6	20.6	70.0	46.6	11.1	41.4	70.5	8.4	20.3
SRJ23	4	2.8	85.9	11.2	16.8	72.0	9.8	14.1	70.7	14.4
	7	6.2	37.1	56.1	46.3	24.4	28.4	60.4	18.4	20.0

J2—late apoptotic/secondary necrotic cells, J3—live cells, J4—early apoptotic cells. Values are mean of two experiments with average difference <10% of the mean value.

involved in G_1 phase (CDK4) and G_2/M phase (CDK1) of MCF-7 cells by employing western blot analysis. Treatment with 1 and 7 μM SRJ09 for 72 h downregulated CDK4 expression without altering the CDK1 expression (Figure 5) and therefore, we concluded G_1 arrest by SRJ09 was very likely to be because of suppression of CDK4. The type of cell cycle arrest induced by andrographolide is controversial. Rajagopal *et al*. (2003) showed andrographolide induced a G_1 arrest through the induction of CDKI (p27) and with a concomitant decrease in CDK4 expression. However, our very own study revealed this compound had a non-phase-specific blockade of the cell cycle progression, whereby it induced both G_1 and S arrest in MCF-7 cells (Jada *et al*., 2003). Interestingly, the three semisynthetic andrographolide derivatives induced G_1 phase-specific cell cycle block in MCF-7 and HCT-116 cells. From this study we concluded SRJ09-induced G_1 arrest most likely through suppression of CDK4 levels, similar to a study by Satyanarayana *et al*. (2004) who showed another semisynthetic derivative of andrographolide, DRF 3188, induced G_1 arrest through down-regulation of CDK-4. However, the exact mechanism of downregulation of CDK4 by andrographolide-related compounds is presently unknown and warrants further investigation.

DNA histograms used for cell cycle analysis consistently showed the presence of apoptotic populations among cells treated with SRJ09 and SRJ23 (Figures 3 and 4). To ascertain that the mode of cell death was by apoptosis, morphological (fluorescence microscopy) and annexin V-FITC/PI—flow cytometry analysis were carried out. The classical apoptotic morphology of nuclear chromatin condensation and fragmentation were noted in HCT-116 cells treated with SRJ09 and SRJ23 (Figure 6). Apoptosis is characterized by distinct biochemical features, in which activation of catabolic processes and enzymes occur before cytolysis, thereby facilitating cell morphological changes, such as PS externalization to the cell surface, mitochondrial alterations, membrane blebbing, cell shrinkage and nuclear condensation/fragmentation (Hotz *et al*., 1994; Hengartner, 2000). Early apoptotic cells tend to exhibit PS on outer cell membrane, which is normally positioned across the inner membrane (Fadok *et al*., 1992) and it has a strong binding affinity to annexin V (Vermes *et al*., 2000). Accordingly, early apoptotic and some late apoptotic cells (commonly known as secondary necrotic cells) can be quantified by flow cytometry assay with fluoresceinated annexin V (annexin V–FITC) and DNA-binding fluorochrome (PI) (Andree *et al*., 1990). Temporary changes in the number of early apoptotic cells, late apoptotic/secondary necrotic cells and live cells were dependent on the test compounds used. Determination of exposure of PS on the cell surface as an early event in HCT-116 cells treated with SRJ09 and SRJ23 was confirmed by annexin V-FITC/PI (Figures 7 and 8). It is well established that agents that are capable of inducing apoptosis as mode of cell death are good anticancer candidates (Makin and Hickman, 2000). Therefore, andrographolide derivatives are potential anticancer candidates that are believed to possess the characteristics of inducing apoptosis selectively in cancer cells. Although the precise molecular mechanisms of cytotoxic activities of the benzylidene derivatives are still ambiguous, the recent finding that v-Src is a molecular target of andrographolide (Liang *et al*., 2008) plus the fact that novel mechanisms of action, based on the NCI *in silico* analyses, have been attributed to these compounds, both encourage the further study of this class of compounds. Presently, studies are underway to further characterize the molecular events leading to cell cycle arrest and apoptosis by SRJ09. In addition, we are exploring the possibilities of modifying the pharmacophores of the lead compound for improvement of the biological activity profile.

Acknowledgements

One of us (SRJ) thanks the European Association for Cancer Research (EACR) for a travel fellowship to carry out the research at The University of Nottingham, Nottingham, United Kingdom. The project was funded by the Malaysian Ministry of Science, Technology and Innovation (MOSTI) under the Intensification of Research in Priority Areas (IRPA) Programme (Grants: 06-02-04-0088 and 06-02-04-0603-EA001). We also thank the NCI Developmental Therapeutics Program for the *in vitro* pharmacological evaluation of compounds.

Conflict of Interest

The authors state no conflict of interest.

References

Andree HA, Reutelingsperger CP, Hauptmann R, Hemker HC, Hermens WT, Willems GM (1990). Binding of vascular anticoagulation alpha (VAC alpha) to planar phospholipid bilayer. *J Biol Chem* **265**: 4923–4928.

Bartek J, Lukas J (2001). Pathways governing G1/S transition and their response to DNA damage. *FEBS Lett* **490**: 117–122.

Basak A, Cooper S, Roberge AG, Banik UK, Chretien M, Seidah NG (1999). Inhibition of proprotein convertases-1, -7 and furin by diterpenes of Andrographis paniculata and their succinoyl esters. *Biochem J* **338**: 107–113.

Bensky D, Gamble A (1993). *Chinese Herbal Medicine: Materia Medica*. Eastland press: CA, USA.

Boyd MR (1989). Status of the NCI preclinical antitumor drug discovery screen: implications for selection of new agents for clinical trials. In: DeVita Jr VT, Hellman S, Rosenberg SA, (eds). *Cancer: Principles and Practice of Oncology*. Lippincott: Philadelphia, PA, **3**: 1–12.

Boyd MR, Paull KD (1995). Some practical considerations and applications of the National Cancer Institute *in vitro* anticancer drug discovery screen. *Drug Develop Res* **34**: 91–109.

Brooks G, Poolman RA, Li JM (1998). Arresting developments in the cardiac myocyte cell cycle: role of cyclin-dependent kinase inhibitors. *Cardiovasc Res* **39**: 301–311.

Chakravarti D, Chakravarti RN (1952). Andrographolide. Part 1. *J Chem Soc* 1697–1700, http://www.rsc.org/publishing/journals/article.asp?doi=JR9520001697.

Cheung HY, Cheung SH, Li J, Cheung CS, Lai WP, Fong WF *et al*. (2005). Andrographolide isolated from Andrographis paniculata induces cell cycle arrest and mitochondrial-mediated apoptosis in human leukemic HL-60 cells. *Planta Med* **71**: 1106–1111.

Chiou WF, Chen CF, Lin JJ (2000). Mechanisms of suppression of inducible nitric oxide synthase (iNOS) expression in RAW 264.7 cells by andrographolide. *Br J Pharmacol* **129**: 1553–1560.

Chiou WF, Lin JJ, Chen CF (1998). Andrographolide suppresses the expression of inducible nitric oxide synthase in macrophage and restores the vasoconstriction in rat aorta treated with lipopolysaccharide. *Br J Pharmacol* **125**: 327–334.

Covell GD, Anders W, Alfred AR, Narmada T (2003). Molecular classification of cancer: unsupervised self-organizing map analysis of gene expression microarray Data. *Mol Cancer Ther* **2**: 317–332.

Fadok VA, Voelker DR, Campbell PA, Cohen J, Bratton DL, Henson PM (1992). Exposure of phosphatidylserine on the surface of apoptotic lymphocytes triggers specific recognition and removal by macrophages. *J Immunol* **148**: 2207–2216.

Hall M, Peters G (1996). Genetic alterations of cyclins, cyclin-dependent kinases, and Cdk inhibitors in human cancer. *Adv Cancer Res* **68**: 67–108.

Harper JW, Elledge SJ (1996). Cdk inhibitors in development and cancer. *Curr Opin Genet Dev* **6**: 56–64.

Hengartner MO (2000). The biochemistry of apoptosis. *Nature* **407**: 770–776.

Hidalgo MA, Romero A, Figueroa J, Cortes P, Concha II, Hancke JL *et al*. (2005). Andrographolide interferes with binding of nuclear factor-κβ to DNA in HL-60-derived neutrophilic cells. *Br J Pharmacol* **144**: 680–686.

Hotz MA, Gong J, Traganos F, Darzynkiewicz Z (1994). Flow cytometric detection of apoptosis: comparison of the assays of *in situ* DNA degradation and chromatin changes. *Cytometry* **15**: 237–244.

Jada SR, Hamzah AS, Lajis NH, Saad MS, Stevens MF, Stanslas J (2006). Semisynthesis and cytotoxic activities of andrographolide analogues. *J Enzyme Inhib Med Chem* **21**: 145–155.

Jada SR, Matthews C, Stevens MF, Stanslas J (2005). Mechanism of antitumour activities of andrographolide derivatives. NCRI Cancer Conference, Birmingham, United Kingdom (2–5 October): P23 (pg. 15).

Jada SR, Stanslas J, Lajis NH, Saad S, Hamzah AS, McCorrel A *et al*. (2003). APAG-1 derivatives as antitumour agents. *Br J Cancer* **88** (Suppl 1): S29 (P17).

Jada SR, Subur GS, Matthews C, Hamzah AS, Lajis NH, Saad MS *et al*. (2007). Semisynthesis and *in vitro* anticancer activities of andrographolide analogues. *Phytochemsitry* **68**: 904–912.

Lee KM, Saiz JE, Barton WA, Fisher RP (1999). Cdc2 activation in fission yeast depends on Mcs6 and Csk1, two partially redundant Cdk-activating kinases (CAKs). *Curr Biol* **9**: 441–444.

Liang FP, Lin CH, Kuo CD, Chao HP, Fu SL (2008). Suppression of v-Src transformation by andrographolide via degradation of the v-Src protein and attenuation of the Erk signaling pathway. *J Biol Chem* **283**: 5023–5033.

Makin G, Hickman JA (2000). Apoptosis and cancer chemotherapy. *Cell Tissue Res* **301**: 143–152.

Matsuda T, Kuroyanagi M, Sugiyama S, Umehara K, Ueno A, Nishi K (1994). Cell differentiation-inducing diterpenes from Andrographis paniculata Nees. *Chem Pharm Bull* **42**: 1216–1225.

Monks A, Scudiero D, Skehan P, Shoemaker R, Paull K, Vistica D *et al*. (1991). Feasibility of a high flux anticancer drug screen using a diverse panel of cultured human tumor cell lines. *J Natl Cancer Inst* **83**: 757–766.

Morgan DO (1995). Principles of CDK regulation. *Nature* **374**: 131–134.

Mosmann T (1983). Rapid colorimetric assay for cellular growth and survival: application to proliferation and cytotoxicity assays. *J Immunol Methods* **65**: 55–63.

Mukherjee AK, Basu S, Sarkar N, Ghosh AC (2001). Advances in cancer therapy with plant based natural products. *Curr Med Chem* **8**: 1467–1486.

Ormerod MG (1999). *Flow Cytometry: A Practical Approach*. Oxford University Press: New York.

Piwnica-Worms H (1999). Cell cycle: fools rush in. *Nature* **401**: 535–536.

Puri A, Saxena R, Saxena RP, Saxena KC, Srivastava V, Tandon JS (1993). Immunostimulant agents from Andrographis paniculata. *J Nat Prod* **56**: 995–999.

Rajagopal S, Kumar RA, Deevi DS, Satyanarayana C, Rajagopalan R (2003). Andrographolide, a potential cancer therapeutic agent isolated from Andrographis paniculata. *J Exp Ther Oncol* **3**: 147–158.

Satyanarayana C, Deevi DS, Rajagopalan R, Srinivas N, Rajagopal S (2004). DRF 3188 a novel semisynthetic analog of andrographolide: cellular response to MCF 7 breast cancer cells. *BMC Cancer* **4**: 1–8.

Sampath D, Plunkett W (2001). Design of new anticancer therapies targeting cell cycle checkpoint pathways. *Curr Opin Oncol* **13**: 484–490.

Shen YC, Chen CF, Chiou WF (2002). Andrographolide prevents oxygen radical production by human neutrophiles: possible mechanism(s) involved in its anti-inflammatory effect. *Br J Pharmacol* **35**: 399–406.

Sherr CJ, Roberts JM (1999). CDK inhibitors: positive and negative regulators of G1-phase progression. *Genes Dev* **13**: 1501–1512.

Siripong P, Konckathip B, Preechanukool K, Picha P, Tunsuwan K, Taylor WC (1992). Cytotoxic diterpenoid constituents from Andrographis paniculata nees leaves. *J Sci Soc Thai* **18**: 187–194.

Stanslas J, Liew PS, Iftikhar N, Lee CP, Saad S, Lajis N *et al*. (2001). Potential of AG in the treatment of breast cancer. *Eur J Cancer* **37** (Suppl. 6): 169.

Tsai HR, Yang LM, Tsai WJ, Chiou WF (2004). Andrographolide acts through inhibition of ERK1/2 and Akt phosphorylation to suppress chemotactic migration. *Eur J Pharmacol* **498**: 45–52.

Vermes I, Haanen C, Reutelingsperger C (2000). Flow cytometry of apoptotic cell death. *J Immunol Methods* **243**: 167–190.

Verpoorte R (1998). Exploration of nature's chemodiversity: the role of secondary metabolites as leads in drug development. *DDT* **3**: 232–238.

Wang T, Liu B, Zhang W, Wilson B, Hong JS (2004). Andrographolide reduces inflammation-mediated dopaminergic neurodegeneration in mesencephalic neuron-glia cultures by inhibiting microglial activation. *J Pharmacol Exp Ther* **308**: 975–983.

Weinstein JN, Mayers TG, O'Conner PM, Friend SH, Forance AJ, Kohn KW *et al*. (1997). An information-intensive

approach to the molecular pharmacology of cancer. *Science* **275**: 343–349.

Woo AY, Waye MM, Tsui SK, Yeung ST, Cheng CH (2008). Andrographolide up-regulates cellular glutathione level and protects cardiomyocytes against hypoxia/reoxygenation injury. *J Pharmacol Exp Ther* **325**: 226–235.

Xia YF, Ye BQ, Li YD, Wang JG, He XJ, Lin X *et al*. (2004). Andrographolide attenuates inflammation by inhibition of NF-kappaB activation through covalent modification of reduced cysteine 62 of p50. *J Immunol* **173**: 4207–4217.

Zhang CY, Tan BK (2000a). Hypotensive activity of aqueous extract of Andrographis paniculata in rats. *Clin Exp Pharmacol Physiol* **23**: 675–678.

Zhang XF, Tan BK (2000b). Antihyperglycemic and anti-oxidant properties of Andrographis paniculata in normal and diabetic rats. *Clin Exp Pharmacol Physiol* **27**: 358–363.

Zhou J, Zhang S, Ong CN, Shen HM (2006). Critical role of pro-apoptotic Bcl-2 family members in andrographolide-induced apoptosis in human cancer cells. *Biochem Pharmacol* **72**: 132–144.